

THE TRANSITION OF A MULTI-DIMENSIONAL LORENZ SYSTEM

Zhong Wenyi (钟文义) and Yang Peicai (杨培才)

Institute of Atmospheric Physics, Academia Sinica, Beijing

Received December 4, 1984

ABSTRACT

A multi-dimensional Lorenz system, which includes thirty-three amplitude equations describing time evolution of convection, is derived from two-dimensional Boussinesq equations by using the Galerkin method. Its transition is studied by numerical solution. It is found that, with Rayleigh number increasing from zero to one hundred, five different types of motion appear one after another as follows: stationary motion, periodic motion, quasiperiodic motion with two-fundamental frequencies, quasi-periodic motion with three fundamental frequencies, and chaotic motion. By comparing with the Lorenz model and Curry's fourteen-dimensional model, it is shown that as retained modes increase, the critical values of transition become larger and the types of bifurcation change. The results of dynamic behavior happen to be in agreement with the IIIa route of the Gollub and Benson experiments.

1. INTRODUCTION

Thermal convection, in which great advances have been made in both theory and experiments in recent years, is of great importance for studying the regular and irregular motions of fluid. In 1963, Lorenz⁽¹⁾ selected the shortest spectral model truncated from two-dimensional convection equations in order to study the predictability of the atmospheric motion and for the first time obtained the strange attractor when the control parameter was taken as $r=28.00$. This discovery inspires scientists to connect chaotic solutions obtained directly from deterministic nonlinear differential equations to turbulence phenomena. Since the 1970's many researchers have extensively and profoundly investigated the Lorenz model in wide ranges of parameters to analyse its types of bifurcation. At the same time, the bifurcations of various nonlinear differential equations, such as the Franceschini's^(2,3) five- and seven-dimensional equations of the plane incompressible Navier-Stokes equations and Yahata's⁽⁴⁾ models of Taylor vortices, have been studied by numerical methods. One of the concerned problems is about the relationship between truncated ordinary differential equations and original partial differential equations. Therefore, some authors have studied the effect of truncation and concluded that types of bifurcation are obviously dependent upon the truncation. Through the computation of his fourteen-dimensional model, Curry⁽⁵⁾ has found a normal Hopf bifurcation which is totally different from that of the Lorenz model. In Curry's model, with r increasing from 0 to 100, solutions change in the following order: fixed points, periodic, double-periodic, quasi-periodic with two independent frequencies, and chaotic. Similar situations have been found in Franceschini's numerical results of seven- and five-dimensional models. Marcus⁽⁶⁾ in the study of convection in a spherical geometry

has indicated that time-dependent solutions may exist if more than one horizontal modes are retained and spurious time-dependent solutions can appear if insufficient horizontal modes are retained.

At least four routes of transition have been discovered in Benard convection experiments by Gollub and Benson^[7] using PDV technique, with the Prandtl number of fluid contained in a box, the aspect ratio of which is large, in the range of 2.5 and 5.0. In their experiments, Gollub and Benson have found a quasi-periodic motion with three distinct fundamental frequencies without broad-band components. McLaughlin and Orszag^[8] in their numerical solutions for the three-dimensional time-dependent Boussinesq equations have shown that solutions containing three or more distinct frequencies do contain broad-band components. However, the Yahata's numerical results of Taylor vortices have shown quasi-periodic motion with three fundamental frequencies without broad-band components. The recent computation carried out by Curry et al.^[9] indicates that under the conditions of adequate spatial and temporal resolutions, the solutions of two-dimensional convection equations show little chaos. The solutions of three-dimensional convection, however, can show much more chaotic behaviour.

In this paper, using the Galerkin method to expand the two-dimensional time-dependent Boussinesq equations, we select a truncated model in which thirty-three time-dependent amplitudes are retained. Putting the same aspect and Prandtl number as in the Lorenz model into the set of thirty-three couple-mode equations, we calculate its numerical solution and compare the numerical results with the Lorenz model, the Curry's fourteen-dimensional model and the Gollub and Benson experiments.

II. MODEL EQUATIONS

According to the Boussinesq approximation, the two-dimensional dimensionless time-dependent convection equations can be written as

$$\begin{aligned} \frac{\partial(\Delta\psi)}{\partial t} &= -\frac{\partial(\psi, \Delta\psi)}{\partial(x, z)} + \sigma\Delta^2\psi + \sigma\frac{\partial\theta}{\partial x}, \\ \frac{\partial\theta}{\partial t} &= -\frac{\partial(\psi, \theta)}{\partial(x, z)} + R\frac{\partial\psi}{\partial x} + \Delta\theta, \end{aligned} \quad (1)$$

where ψ is the flow function, θ is the deviation of temperature from the conduction profile, σ is the Prandtl number, R is the Rayleigh number, and $\partial(\phi, \psi)/\partial(x, z)$ represents the Jacobian. The periodic boundary conditions in the horizontal directions and the free boundary conditions in the vertical directions are taken as follows

$$\begin{aligned} \theta &= 0, & (z=0, \pi), \\ \psi &= \Delta\psi = 0, & (z=0, \pi). \end{aligned}$$

If M sine modes and $M+1$ cosine modes in the horizontal directions and N sine modes in the vertical directions are chosen, the Galerkin expansion is expressed as

$$\begin{aligned} \psi(x, z, t) &= \sum_{m=1}^M \sum_{n=1}^N \psi_{m,n}(t) \sin(amx) \sin(nz), \\ \theta(x, z, t) &= \sum_{m=0}^M \sum_{n=1}^N \theta_{m,n}(t) \cos(amx) \sin(nz), \end{aligned} \quad (2)$$

where a is the geometric parameter. The boundary conditions are automatically satisfied.

Substituting (2) into (1), we obtain

$$\begin{aligned} & \sum_{m=1}^M \sum_{n=1}^N \dot{\psi}_{m,n} [-(a^2 m^2 + n^2)] \sin(amx) \sin(nz) \\ &= a \sum_{m=1}^M \sum_{n=1}^N \sum_{k=1}^M \sum_{l=1}^N \psi_{m,n} \psi_{k,l} (a^2 k^2 + l^2) [ml \cos amx \sin nz \cos akx \cos lz \\ & \quad - nk \sin amx \cos nz \cos akx \sin lz] + \sigma \sum_{m=1}^M \sum_{n=1}^N \psi_{m,n} (a^2 m^2 + n^2) \sin amx \sin nz \\ & \quad - \sigma a \sum_{m=0}^M \sum_{n=1}^N \theta_{m,n} \sin amx \sin nz, \end{aligned} \tag{2a}$$

$$\begin{aligned} & \sum_{m=0}^M \sum_{n=1}^N \dot{\theta}_{m,n} \cos amx \sin nz = -a \sum_{n=1}^N \sum_{k=0}^M \sum_{l=1}^N \psi_{m,n} \theta_{k,l} \\ & \quad \times [ml \cos amx \sin nz \cos akx \cos lz + nk \sin amx \cos nz \sin akx \sin lz] \\ & \quad + Ra \sum_{m=1}^M \sum_{n=1}^N m \psi_{m,n} \cos amx \sin nz - \sum_{m=0}^M \sum_{n=1}^N \theta_{m,n} (a^2 m^2 + n^2) \cos amx \sin nz. \end{aligned} \tag{2b}$$

Multiplying Eq. (2a) by $\sin apx \sin qx$, Eq. (2b) by $\cos apx \sin qx$ and integrating them from 0 to $2\pi/a$ for x and from 0 to π for z , we obtain

$$\begin{aligned} \dot{\psi}_{p,q} &= -\frac{a}{4} \cdot \frac{1}{a^2 p^2 + q^2} \sum_{m=1}^M \sum_{n=1}^N \sum_{k=1}^M \sum_{l=1}^N \psi_{m,n} \psi_{k,l} (a^2 k^2 + l^2) (ml I_{m k p}^{(1)} I_{l n q}^{(1)} \\ & \quad - nk I_{k m p}^{(1)} I_{l n q}^{(1)}) - \sigma (a^2 p^2 + q^2) \psi_{p,q} + \sigma a \frac{p}{a^2 p^2 + q^2} \theta_{p,q}, \\ \dot{\theta}_{p,q} &= -\frac{a}{4} \sum_{m=1}^M \sum_{n=1}^N \sum_{k=0}^M \sum_{l=1}^N \psi_{m,n} \theta_{k,l} (ml I_{m k p}^{(2)} I_{l n q}^{(1)} + nk I_{p m k}^{(1)} I_{l n q}^{(1)}) \\ & \quad + a p R \psi_{p,q} - (a^2 p^2 + q^2) \theta_{p,q}, \end{aligned} \tag{3}$$

where

$$I_{m k p}^{(1)} = \begin{cases} -1, & m = k + p \neq 0, \\ 1, & m = |k - p| \neq 0 \text{ or } m = k - p = 0, \\ 0, & \text{the others,} \end{cases}$$

$$I_{m k p}^{(2)} = \begin{cases} 1, & m = k + p \neq 0 \text{ or } m = |k - p| \neq 0 \text{ or } p = m - k = 0, \\ 0, & \text{the others.} \end{cases}$$

When $M=5, N=6$, the truncated model contain thirty-three independent variables, and the set of selected amplitudes is

$$A = \{(0, 2), (1, 1), (0, 4), (1, 3), (2, 2), (3, 1), (0, 6), (1, 5), (2, 4), (3, 3), (4, 2), (5, 1), (2, 6), (3, 5), (4, 4), (5, 3), (4, 6), (5, 5)\}.$$

When $M=1, N=2$, we have the Lorenz model; when $M=3, N=4$, then we obtain the Curry's fourteen-dimensional model. Therefore the thirty-three-dimensional model is a generalization of the Lorenz and Curry's fourteen-dimensional models.

III. NUMERICAL RESULTS

In this section the numerical results obtained by integrating Eq. (3) ($M=5, N=6$) are presented. For all our selected values of parameter $r=R/R_c$ ($R_c=6.75$), the initial values of

all amplitudes are taken to be zero except $\theta_{11}(0)=1$. The power spectra are calculated via FFT of the digital time sequences obtained for several amplitudes and for $\sum_{i=1}^{15} \psi_{p,q}$ and $\sum_{i=16}^{33} \theta_{p,q}$.

Based on the Curry's computation (1978), we consider some values of r in the range of $46.00 < r < 100.00$ to investigate the qualitative properties of solutions. Although it is difficult to determine accurately the critical points of transition, the type of bifurcation in the considered range of r may be obtained.

The steady motion occurs over a wider range of r in the thirty-three-dimensional case than in Curry's fourteen-dimensional case, and stationary solutions continuously exist up to $r=72.00$. The trajectories describing the state of motion are attracted to a fixed point of the thirty-three-dimensional phase space. Fig. 1 shows the development of the amplitude ψ_{11} and the projections of the trajectory on the phase planes (ψ_{11}, θ_{11}) and $(\theta_{02}, \theta_{11})$ at $r=72.00$.

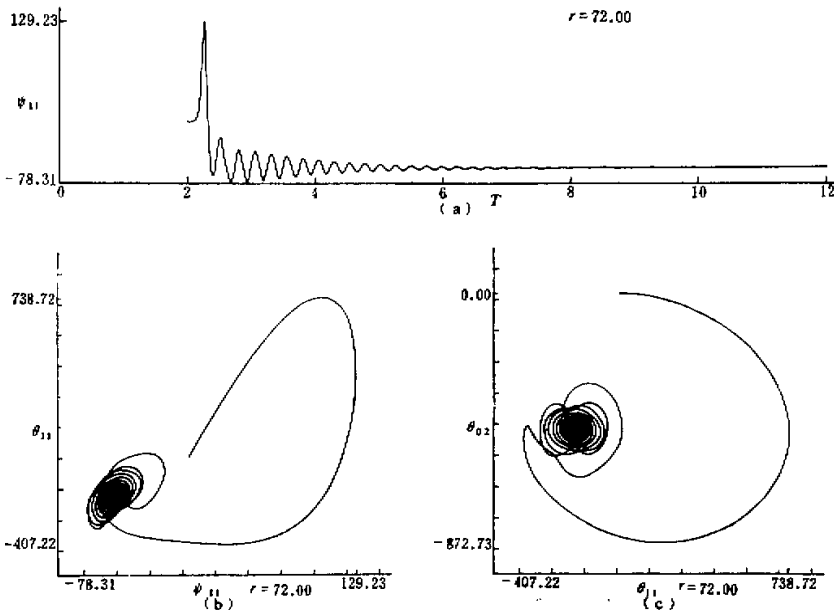


Fig. 1. Stationary solution at $r=72.00$: (a) the development of amplitude ψ_{11} ; (b) and (c) projections of trajectory on the phase planes (ψ_{11}, θ_{11}) and $(\theta_{02}, \theta_{11})$.

Stable periodic motions are obtained at $r=72.29$ and $r=72.76$. The period T is about 0.02990 and the corresponding frequency f_1 is about 33.4472 at $r=72.76$ (Fig. 2). It is found later that frequency f_1 changes a little and remains as a dominant component in the power spectra as r increasing, but its subharmonic frequencies has never been found, indicating that there is no stable double periodic solutions in this interval of parameter.

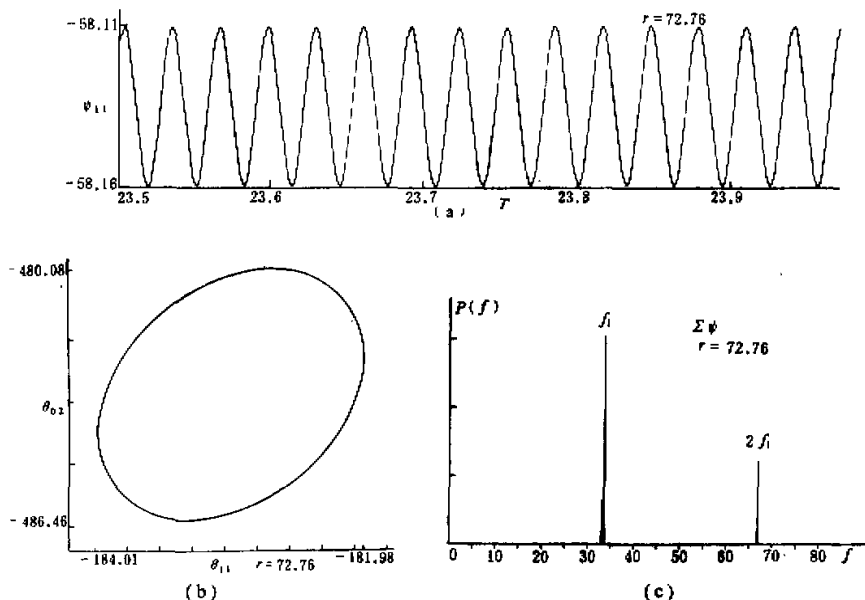


Fig. 2. Periodic motion at $r=72.76$: (a) the development of amplitude ψ_{11} ; (b) the projections of trajectory on phase planes $(\theta_{02}, \theta_{11})$; and (c) the power spectral densities for $\Sigma\psi$.

In the power spectra at $r=73.52$ and $r=74.00$ we find two fundamental frequencies, $f_1 \approx 33.6913$ and $f_2 \approx 19.6533$, and all the other spectral lines can be expressed in terms of the linear combination of f_1 and f_2 with not very large integer coefficients. Moreover, the value of ratio f_1/f_2 varies slightly with r , from 1.713 at $r=73.52$ to 1.720 at $r=74.00$. This indicates that these two frequencies are incommensurable at some values of r in this parameter interval (Fig. 3). In the interval of r from $r=75.00$ to $r=76.00$ we choose three values of parameter to calculate the numerical solutions and find a new frequency $f_3 \approx 4.4$ in the power spectra, and all the spectral lines can be expressed by the linear combination of f_1 , f_2 and f_3 with not very large integer coefficients.

The power-spectral densities at $r=75.00$ show that the third fundamental frequency, $f_3 \approx 4.3945$, is first found in the time development of amplitudes of a few shortwaves. However f_3 does not appear in some longwaves (Fig. 4). On the other hand, the third fundamental frequency appears obviously in all amplitude spectra at $r=76.00$. Moreover, the power spectrum at $r=76.00$ seems to be less broadening than that at $r=75.00$, and the structure of trajectory in the phase space is more regular and different from those when $r=74.00$ and $r=75.00$ (Fig. 5). Table 1 indicates that the ratios of each pair of the three frequencies f_1 , f_2 and f_3 change slightly so that three incommensurable frequencies may exist simultaneously in this parameter interval. This result is slightly different from the picture presented by Newhouse, Ruelle and Takens⁽¹¹⁾ (1978). From the above result we can find that the process from the first appearance of the third fundamental frequency to its stabilizing seems to show a transitional process from a state with higher order to one with lower order and again to another state with higher order.

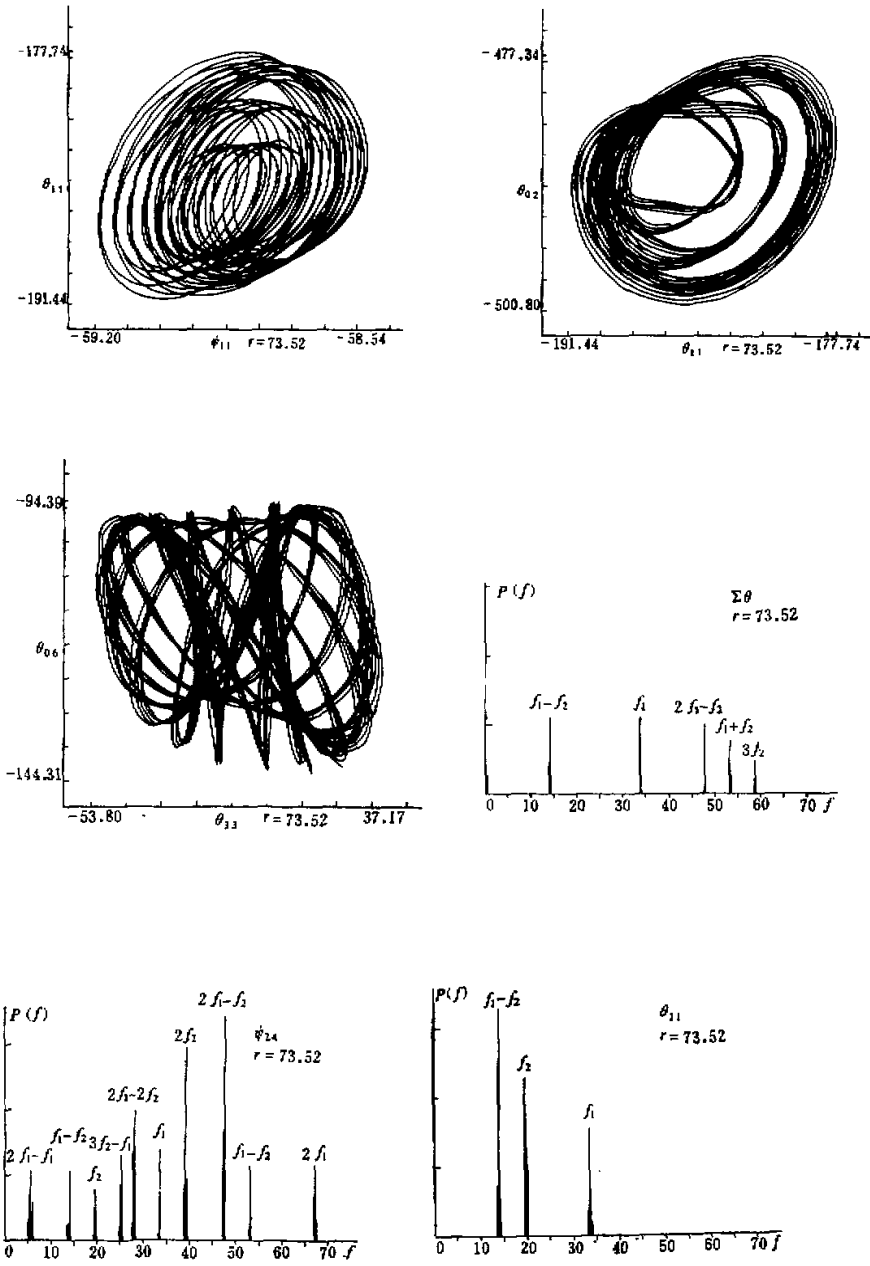


Fig. 3. Quasi-periodic motion with two fundamental frequencies at $r=73.52$: (a) trajectory projections on phase planes (ψ_{11}, θ_{11}) (top left), (θ_{11}, θ_2) (top right), and $(\theta_{33}, \theta_{06})$ (middle left); (b) the power spectral densities for $\Sigma\theta$ (middle right), ψ_{24} (bottom left), θ_{11} (bottom right).

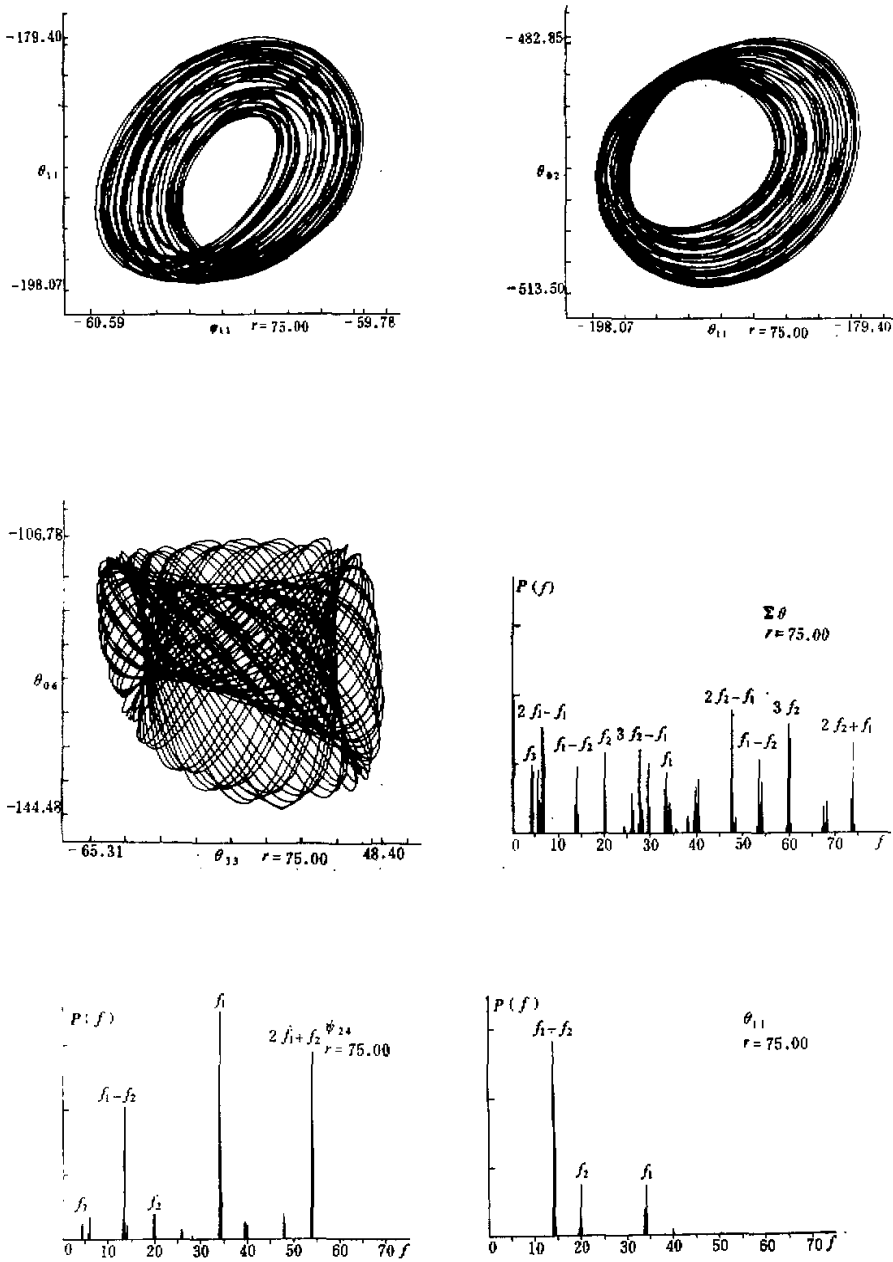


Fig. 4. Quasi-periodic motion with three fundamental frequencies at $r=75.00$: (a) the projections of trajectory on (ψ_{11}, θ_{11}) (top left), $(\theta_{11}, \theta_{01})$ (top right), and $(\theta_{33}, \theta_{04})$ (middle left); (b) the power spectral densities for: $\Sigma \theta$ (middle right), ψ_{01} (bottom left), and θ_{11} (bottom right).

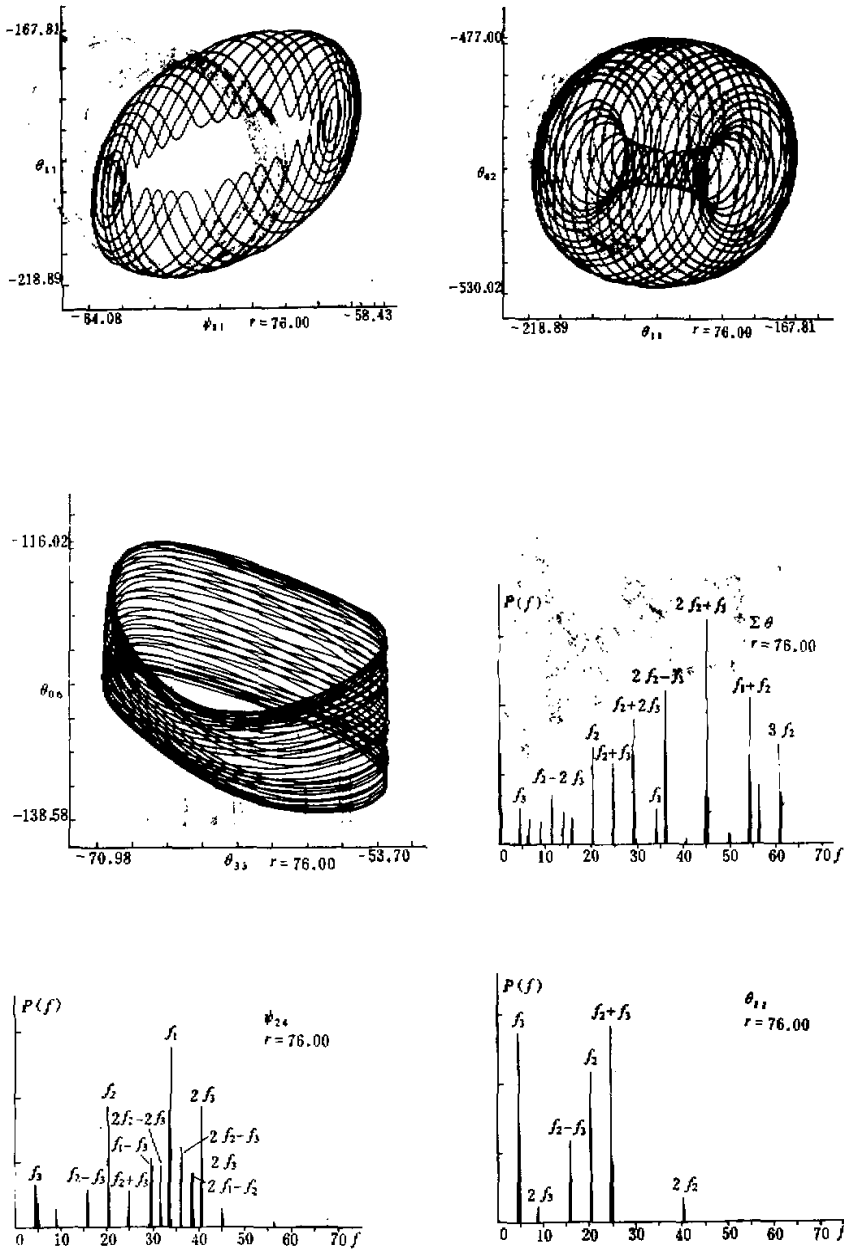


Fig. 5. Quasi-periodic motion with three fundamental frequencies at $r=76.00$: (a) the projections of trajectory on (ψ_{11}, θ_{11}) (top left), $(\theta_{11}, \theta_{21})$ (top right) and $(\theta_{31}, \theta_{41})$ (middle left); (b) the power spectral densities for $\Sigma \theta$ (middle right), ψ_{21} (bottom left) and θ_{11} (bottom right).

Table 1. The Ratios of Each Pair of the Three Frequencies

r	f_1/f_2	f_1/f_3	f_2/f_3
75.00	1.6768	7.6389	4.5556
75.62	1.6908	7.7500	4.5834
76.00	1.6807	7.7500	4.6111

In the interval from $r=77.00$ to $r=79.00$ we choose three values to calculate, and the results are similar to each other in which obvious broad-bands exist in the spectra and the components of spectral bands become more and more complex. In the time development of amplitudes at all the three values of parameter there is an oscillation with a low frequency f_L , which is about 0.24414 when $r=79.00$. This frequency is likely to contain larger errors because the number of samples we choose for spectral analysis is too small to determine accurately such a low frequency. However, we may conjecture that it is these lower frequencies that lead to the broadening of spectral lines in the power spectral densities (Fig. 6).

When $r=80.00$ we obtain a chaotic solution, in which the projections on the (ψ_{11}, θ_{11}) and $(\theta_{11}, \theta_{55})$ phase planes are somewhat similar to the Lorenz strange attractor. The trajectory run back and forth between both attractive basins. The corresponding power spectra become continuous spectra. The result at $r=100.00$ is similar to that at $r=80.00$ (Fig. 7).

Table 2 gives the mean square values of adjacent maxima and minima of amplitudes $\psi_{11}, \psi_{55}, \theta_{11}$ and θ_{55} when time t becomes very large.

Table 2. The Values of $\bar{\psi}_{11}^2$, $\bar{\psi}_{55}^2$, $\bar{\theta}_{11}^2$ and $\bar{\theta}_{55}^2$

r	72.00	72.76	73.52	75.00	78.00	80.00
$\bar{\psi}_{11}^2$	3342	3379	3454	3617	3734	3733
$\bar{\psi}_{55}^2$	3485×10^{-7}	1764×10^6	2551×10^{-6}	2591×10^{-6}	4527×10^{-6}	5379×10^{-6}
$\bar{\theta}_{11}^2$	3313×10^1	3349×10^1	3428×10^1	3583×10^1	4893×10^1	6081×10^1
$\bar{\theta}_{55}^2$	1154×10^{-1}	3512×10^{-1}	4628×10^{-1}	5920×10^{-1}	7755×10^{-1}	7088×10^{-1}

From the above results we can obtain a bar diagram which shows the route to chaos. Four bar diagrams, the Lorenz, the Curry fourteen-dimensional model, the thirty-three-dimensional model, and the IIIa route of the Gollub and Benson experiments are given in Fig. 8 in order to compare their transitions.

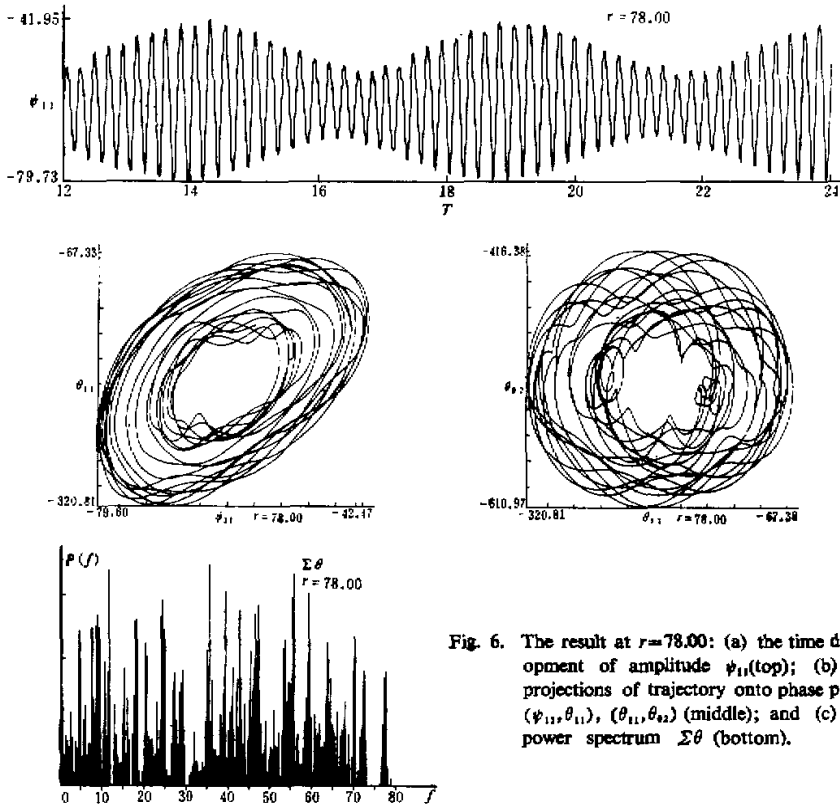


Fig. 6. The result at $r=78.00$: (a) the time development of amplitude ψ_{11} (top); (b) the projections of trajectory onto phase planes $(\psi_{11}, \theta_{11}), (\theta_{11}, \theta_{12})$ (middle); and (c) the power spectrum $\Sigma \theta$ (bottom).

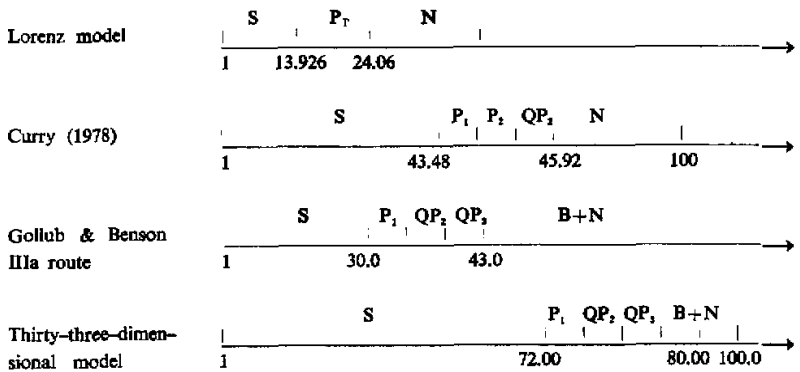
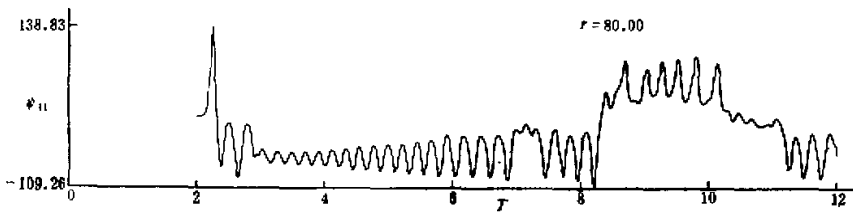
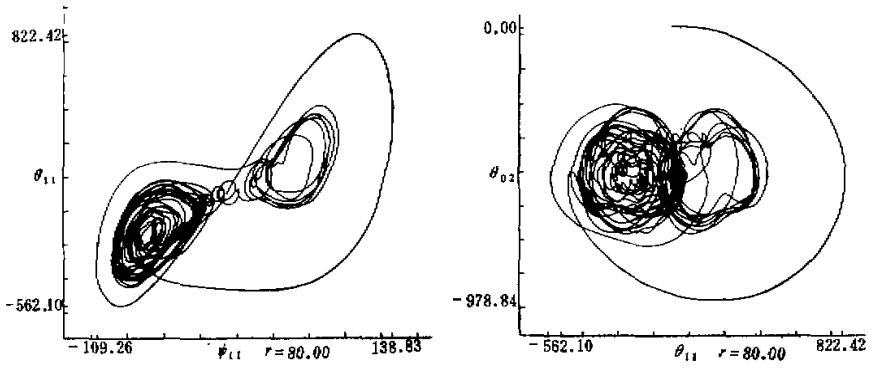


Fig. 8. Bar diagrams.

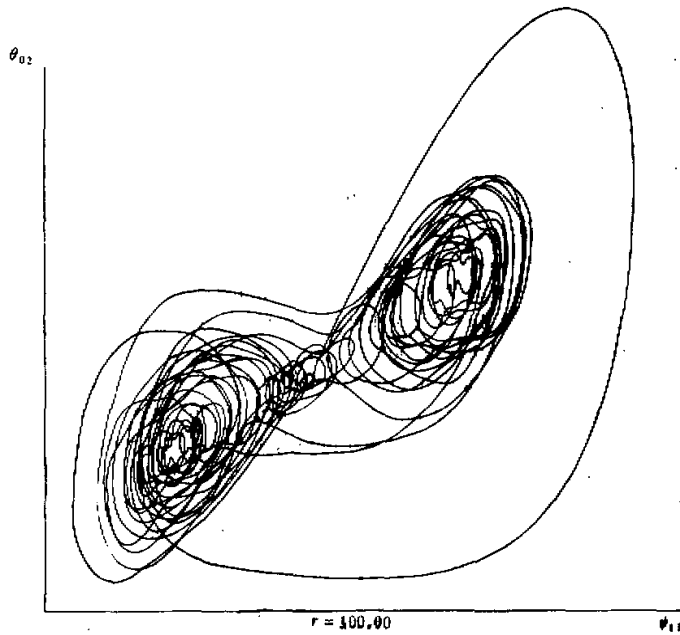
S represents the steady motion; P_T the perturbation; P₁ the periodic motion; P₂ the periodic motion with double period; QP₂ the quasi-periodic motion with three fundamental frequencies; QP₃ the quasi-periodic motion with three fundamental frequencies; B the motions including broad-bands in their power spectra; and N the chaotic motion.



(a)



(b)



(c)

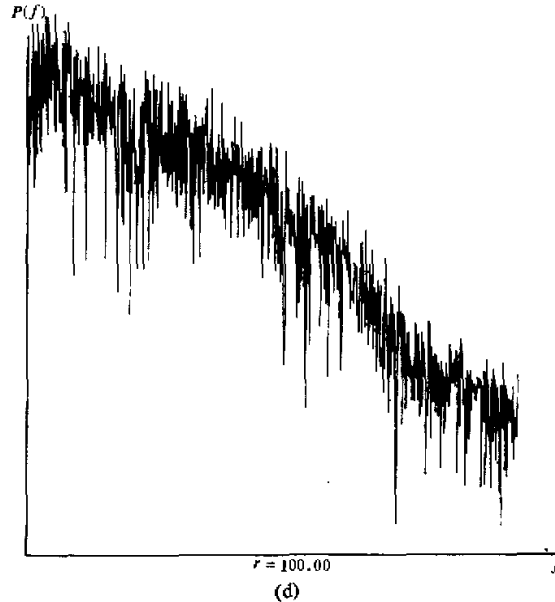


Fig. 7. The Chaotic motion at $r=80.00$ and $r=100.00$: (a) the time development of amplitude ψ_{11} at $r=80.00$; (b) the projections of trajectory on phase planes (ψ_{11}, θ_{11}) and $(\theta_{11}, \theta_{21})$, at $r=80.00$; (c) and (d) the projection of trajectory at $r=100.00$ and the power spectrum.

IV. SUMMARY AND DISCUSSION

(1) Comparing the numerical results of the thirty-three-dimensional model with those of Lorenz model and of Curry's fourteen-dimensional model, it can be seen that the critical parameter values of transition become larger as the number of retained spectral modes increases. This means that if the spacial resolution of retained modes is not adequate, then spurious time-dependent solutions may appear (including chaotic solutions). This result is consistent with that of Marcus. This can be explained by the fact that those additional small-scale modes obstruct the development of motion to irregular motion. However, is there a limit to these critical parameter values when the remained spectral modes increase? According to the above explanation we may hypothesize that it is possible that the infinite degree of freedom may shift the chaotic motion up to an infinitely great parameter value. Because of the limitation of computer we were not able to calculate larger models. After finishing the computation of the thirty-three-dimensional model, we read the much larger-scale computed results obtained by Curry et al. which have answered some questions of ours. Thus, it can be seen that the chaotic solutions computed from the Lorenz model, the Curry's fourteen-dimensional model and the thirty-three-dimensional model may be regarded as the results of serious truncations. It is still not really proved that chaotic solutions can be obtained directly from general two-dimensional Benard convection equations.

(2) The results of the thirty-three-dimensional model, the Lorenz model and the Curry's fourteen-dimensional model indicate that computed time-dependent solutions are all in the

attractive regions around two fixed points. Increase of the remained modes does not change this kind of property. Therefore, selecting appropriate modes, one can estimate the quantitative properties of the transition from the conductive state to the steady convection state by means of finding the first- and second-order bifurcations of simple spectral models.

Comparing the energies of various waves in the thirty-three-dimensional model with each other we can see that the energies contained in the large-scale waves are much higher than those in the small-scale waves. Their energies decay almost exponentially with the decrease of the scales of waves (see Table 2). This indicates that although the energies in the small-scale waves amount to a very small portion of the total energy, they play an important role in changing higher-order bifurcation and critical parameter values through the nonlinear feedback function.

(3) From the power spectra of time series of amplitudes we find that with the increase of r the third independent fundamental frequency appears first in the amplitudes of short-waves, indicating that this kind of change of the system begins first in certain individual short-waves.

The power-spectrum analyses show that, in general, with the same value of r , all amplitudes show the same behaviour, that is, include the same oscillating frequencies, but the intensity of each frequency in distinct amplitudes may be different. The peaks of a specific frequency are relatively higher in the power spectra of some amplitudes but relatively lower in the power spectra of the other amplitudes. For some values of parameter, it is possible that a certain frequency appears only in the power spectrum of individual amplitude and is not found in other amplitudes. With r increasing, one may find this frequency in the power spectra of all amplitudes. This may be interpreted as that a new oscillation is firstly excited in a specific amplitude and the function of nonlinearity is to restrict the infinite development of the oscillation, to stabilize it, and to propagate it to all amplitudes.

(4) The computed results of the thirty-three-dimensional model happen to be qualitatively in agreement with the third route of the Gollub and Benson experiments.

We would like to thank Professors Zhou Xiuji and Hao Bolin for advice and assistance on the research work and Mr. Zou Chengzhi for discussion.

REFERENCES

- [1] Lorenz, E. N., *J. Atmos. Sci.*, 20(1963), 130—141.
- [2] Boldrighini, C. and Franceschini, V., *Commun. Math. Phys.*, 64(1979), 159—170.
- [3] Franceschini, V. and Tebaldi, C., *J. Stat. Phys.*, 25(1981), 397—417.
- [4] Yahata, H., *Prog. Theor. Phys.*, 61(1979), 791—799. 64(1980), 782—793.
- [5] Curry, J. H., *Commun. Math. Phys.*, 60(1978), 193—204.
- [6] Marcus, P.S., *J. Fluid Mech.*, 103(1981), 241—255.
- [7] Gollub, J. P. and Benson, S. H., *J. Fluid Mech.*, 100(1980), 449—470.
- [8] McLaughlin, J. B. and Orszag, S. A., *J. Fluid Mech.*, 122(1982), 123—142.
- [9] Curry, J. H., Herring, J. R., Loncaric, J. and Orszag, S.A., *J. Fluid Mech.*, 147(1984), 1—38.
- [10] Ruelle, D., Takens, F. and Newhouse, S. E., *Commun. Math. Phys.*, 64(1978), 35—40.